Islands appear to generate much complexity. Furthermore, intense tidal flows make this a region of turbulent mixing.

The West Wind Drift and Zeehan Current

The continental shelf south of Australia is nearly 200 km wide along much of its length. Circulation north of the shelf break is generally quite slow; the West Wind Drift is strongest in a narrow jet along the shelf break, particularly in winter where speeds reach 1 m s^{-1}. Strong eddy formation also occurs at the south edge of the Leeuwin Current/West Wind Drift south of Australia (**Figure 4**). Similar eddies occur in the Leeuwin Current off Australia's west coast (not shown). Strong evaporation occurs in the Great Australian Bight in summer. Much of the salty water so generated flows eastward in winter, through Bass Strait; it sinks some 400 m on encountering the warm, light waters of the East Australian Current in eastern Bass Strait. However, satellite-tracked buoys frequently arc south-eastward to join the Zeehan Current, usually staying close to the shelf break in the process. These flows are slower than those found off Cape Leeuwin, but current meter moorings in the Zeehan Current show it to be much deeper than the Leeuwin Current. The Zeehan Current extends down to 1000 m in winter. The summer upwelling referred to earlier appears to be mainly confined to the narrow continental shelf region off western Victoria; it occurs during bursts of easterly wind.

See also

East Australian Current. El Niño Southern Oscillation (ENSO). Indian Ocean Equatorial Currents.

Further Reading

Cresswell GR and Golding TJ (1980) Observations of a south-flowing current in the southeastern Indian Ocean. *Deep Sea Research* 27A: 449–466.

Cresswell GR (1991) The Leeuwin Current – observations and recent models. *Journal of the Royal Society of Western Australia* 74: 1–14.

Godfrey JS (1996) The effect of the Indonesian Throughflow on ocean circulation and heat exchange with the atmosphere: A review. *Journal of Geophysical Research* 101: 12 217–12 238

Meyers G (1996) Variation of Indonesian Throughflow and the El Niño–Southern Oscillation. *Journal of Geophysical Research* 101: 12 255–12 263.

Murray SP and Arief D (1988) Throughflow into the Indian Ocean through the Lombok Strait, January 1985–January 1986. *Nature* 133: 444–447.

Smith RL, Huyer A, Godfrey JS and Church JA (1991) The Leeuwin Current off Western Australia, 1986–1987. *Journal of Physical Oceanography* 21: 323–345.

INHERENT OPTICAL PROPERTIES AND IRRADIANCE

T. D. Dickey, University of California, Santa Barbara, CA, USA

doi:10.1006/rwos.2001.0318

Introduction

Light is of great importance for the physics, chemistry, and biology of the oceans. In this article, a brief introduction is provided to the two subdisciplines focusing on light in the ocean: ocean optics and bio-optics. A few of the problems addressed by these subdisciplines are described. Several of the *in situ* sensors and systems used for observing the subsurface light field and optical properties are introduced along with general explanations of the operating principles for measuring optical variability in the ocean. Some of the more commonly used ocean platforms and optical systems are also discussed. Finally, some examples of oceanographic optical data sets are illustrated.

Solar radiation, which includes visible radiation or light, impinges on the surface of the ocean. On average, a small fraction or percentage is reflected back into the atmosphere (roughly 6% on average) while a high fraction penetrates into the ocean. This fraction (or percentage), defined as the albedo, varies in time and space as a function of several factors including solar elevation, wave state, surface roughness, foam, and whitecaps. Radiative transfer is a branch of oceanography termed 'ocean optics,' a term that denotes studies of light and its propagation through the ocean medium. Radiative transfer processes depend on the optical properties of the components lying between the radiant source (e.g., the sun) and the radiation sink (the ocean and its constituents). Another commonly used term is 'bio-optics,' which invokes the notion of biological effects on optical properties and light

propagation and vice versa. Some of the data used for examples here focus on bio-optical and physical interactions.

Solar radiation spans a broad range of the electromagnetic energy spectrum. The visible portion, roughly 400–700 nm, is of primary concern for ocean optics for many practical problems. These include: underwater visibility, photosynthesis and primary production of phytoplankton, upper ocean ecology, red tides, pollution, biogeochemistry including carbon cycling, photochemistry, light-keyed migration of organisms, heating of the oceans, global climate change, and remote sensing of ocean color. It is worth noting that optical oceanographers are also interested in the ultraviolet (UV) range and the infrared. For example, UV radiation can damage phytoplankton and can also lead to modifications in genetic material, and thus evolution, whereas the penetration of the infrared is critical for near surface radiant heating.

Solar radiation is clearly a primary driver for ocean physics, chemistry, and biology as well as their complex interactions. Thus, it is not surprising that virtually all important oceanographic problems require interdisciplinary approaches and necessarily atmospheric, physical, chemical, biological, optical, and geological data sets. These data sets should be collected concurrently (concept of synopticity) and span sufficient time and space scales to observe the relevant processes of interest. For local studies involving optics, variability at timescales of one day and one year are especially important. For global problems, variability extends well over ten orders of magnitude in space [O(millimeters) to O(10^4 kilometers)] and much longer in time for climate problems. Multiplatform observing approaches are essential. Capabilities for obtaining atmospheric and physical oceanographic data are relatively well advanced in contrast to those for chemical, biological, optical, acoustical, and geological data. This is not surprising, because of the greater complexity and nonconservative nature of the chemistry and biology of the oceans. Yet, remarkable advances are being made in these areas as well. In fact, several bio-optical, chemical, geological, and acoustical variables can now be measured on the same time and space scales as physical variables; however many more variables still need to be measured.

Fundamentals of Ocean Optics

A few operation definitions need to be introduced before discussing the various optical sensors. Light entering the ocean can be absorbed or scattered. The details of these processes comprise much of the study of ocean optics. First, it is convenient to classify bulk optical properties of the ocean as either inherent or apparent. Inherent optical properties (IOPs) depend only on the medium and are independent of the ambient light field and its geometrical distribution. Inherent optical properties include: spectral absorption coefficient, $a(\lambda)$, spectral scattering coefficient, $b(\lambda)$, and spectral beam attenuation coefficient (or, sometimes denoted as 'beam c'), $c(\lambda)$. To define these coefficients, consider a beam of monochromatic light impinging perpendicularly on a thin layer of water. The fraction of the incident radiant flux, Φ_0 (energy or quanta per unit time), which is absorbed by the medium, Φ_a/Φ_0, divided by the thickness of the layer is the absorption coefficient, a, in units of m^{-1}. Similarly, the analogous scattering coefficient, b (m^{-1}) is the fraction of the incident radiant flux scattered from its original path (primarily forward), Φ_b/Φ_0, divided by the thickness of the layer. The beam attenuation coefficient is simply $c = a + b$.

The spectral volume scattering function, $\beta(\psi, \lambda)$ represents the scattered intensity of light per unit incident irradiance per unit volume of water at some angle ψ (with respect to the exiting, nonscattered incident beam) into solid angle element $\Delta\Omega$. Units for $\beta(\psi,\lambda)$ are $m^{-1}\ sr^{-1}$. This is essentially the differential scattering cross-section per unit volume in the parlance of nuclear physics. The spectral scattering coefficient is obtained by integrating the volume scattering function over all directions (solid angles). The forward scattering coefficient, b_f, is obtained by integrating over the forward-looking hemisphere ($\psi = 0$ to $\pi/2$) and the backward scattering coefficient, b_b, is calculated by integrating the back-looking hemisphere ($\psi = \pi/2$ to π). The spectral volume scattering phase function is the ratio of $\beta(\psi, \lambda)$ to $b(\lambda)$ with units of sr^{-1}. Other important IOPs include spectral single-scattering albedo, $\omega_0(\lambda) = b(\lambda)/c(\lambda)$, and fluorescence, which can be considered a special case of scattering. (Note: fluorescence is not strictly an IOP; however it is often used as a proxy for chlorophylla). The proportion of light which is scattered versus absorbed is characterized by $\omega_0(\lambda)$; that is, if scattering prevails then $\omega_0(\lambda)$ approaches a value of 1 and if absorption dominates, $\omega_0(\lambda)$ approaches 0.

IOPs obey simple mathematical operations. For many applications, it is often convenient to partition the total absorption coefficient, $a_t(\lambda)$, the total scattering coefficient, $b_t(\lambda)$, and the total beam attenuation coefficient, $c_t(\lambda)$, in terms of contributing constituents such that:

$$a_t(\lambda) = a_w(\lambda) + a_{ph}(\lambda) + a_d(l) + a_g(\lambda) \qquad [1]$$

$$b_t(\lambda) = b_w(\lambda) + b_{ph}(\lambda) + b_d(\lambda) + b_g(\lambda) \quad [2]$$

$$c_t(\lambda) = c_w(\lambda) + c_{ph}(\lambda) + c_d(\lambda) + c_g(\lambda) \quad [3]$$

The subscripts indicate contributions by pure sea water (w), phytoplankton (ph), detritus (d), and gelbstoff (g) with units of m^{-1} for all variables. Detritus is the term for particulate organic debris (e.g., fecal material, plant and animal fragments, etc.) and gelbstoff (sometimes called yellow matter or gilvin) is the term for optically active dissolved organic material. Note that eqns [1]–[3] are intended for use where bottom and coastal sediment contributions are minimal. The spectral absorption coefficient of pure sea water is well characterized and is nearly constant in space and time with greater absorption in the red than blue portions of the visible spectrum. The magnitudes of the detrital and gelbstoff absorption spectra tend to decrease monotonically with increasing wavelength and can be modeled. Phytoplankton spectral absorption varies significantly in relation to community composition and environmental changes; however characteristic peaks are typically found near wavelengths of 440 nm and 683 nm. Much bio-optics research focuses on the temporal and spatial variability of $a_{ph}(\lambda)$. Ship-based ocean water samples have often been used for studies of the IOPs, however, it is quite preferable to obtain *in situ* measurements to insure representative local values as well as to characterize temporal and spatial variability, preferably with simultaneous physical, chemical, and biological measurements.

Instrumentation

Beam transmissometers have been the most commonly used instruments for measuring IOPs with a variety of applications ranging from determinations of suspended sediment volume to phytoplankton biomass and productivity to particulate organic carbon (POC). The principle of operation involves the measurement of the proportion of an emitted beam, C, which is lost through both absorption and scattering as it passes to a detector through some pathlength ΔL. The beam attenuation coefficient, c, is then given as $-[\ln(1-C)]/\Delta L$; or light intensity, I, is given as $I(\Delta L) = I(0)\ \exp(-c\ \Delta L)$. Similar expressions apply for absorption coefficient, a, and scattering coefficient, b. Beam transmissometers have often used a red light emitting diode (660 nm) for the collimated light source and pathlengths of 25 or 100 cm (long pathlengths are preferable for clearer waters). The wavelength of 660 nm was selected in order to minimize attenuation by gelbstoff, which attenuates strongly at shorter wavelengths but minimally in the red. One of the measurement complications for beam c is that most scattering in ocean waters is in the forward direction. The acceptance angle of the detector is thus made as small as possible (< 1–2°) to minimize underestimation of beam c. Corrections are done for this effect as well as for instrument temperature and pressure effects.

In situ multispectral attenuation–absorption (ac-meters) instruments have recently become commercially available. These concurrently measure spectral absorption and attenuation coefficients, which are spectral signatures of both particulate and dissolved material. These devices use dual light sources and interference filters on a single rotating wheel (nine wavelengths from 400 to 715 nm with 10 nm bandwidth). Whereas earlier beam transmissometers were open to sea water, the newer ac-meters use two tubes through which sea water is pumped. The inside of the c-tube is flat black to minimize reflections whereas the a-tube is reflective (shiny) in order to maximize internal reflection to better estimate absorption. The deployment of these meters requires minimal lateral and torsional stressing in mounting (sensitivity of beam alignment) and good flow through the tubes. Calibrations involve temperature, salinity, and pure water measurements. A correction is also needed to account for the fact that not all scattered light is collected (causing a biased over-estimate of absorption).

Similar, though more capable instruments, have recently been developed to measure a and c at 100 wavelengths from 400 to 726 nm wavelengths with 3.3 nm resolution. A single white light source is used with fiberoptics to provide light to each of the two tubes (for a and b) as well as for a reference path (for correcting changes in lamp output). Each light path has its own spectrometer (using a 256 pixel photodiode array). Biofouling is an issue for all optical instruments. Closed (pumped) systems are less susceptible to fouling as they are primarily in the dark. A variety of special antifouling methods have been attempted with mixed success. These have included copper screens, copper flow tubes, bromide solutions, and other cleaning agents. Spectral scattering coefficient can be computed from ac-meter data by simply performing the difference $b = c - a$. Spectral a–c meter data and relevant spectral decomposition models can be used to provide *in situ* estimates of $a_{ph}(\lambda)$ and other components (e.g., gelbstoff) for a broad range of environmental conditions as a function of time at fixed depths using moorings or as a function

of depth from ships or profilers deployed from moorings.

The volume scattering function is one of the more important and challenging measurements of optical oceanography. Until recently, few instruments existed for this measurement and data collected with an instrument developed in the 1970s were commonly used for many problems. The challenge arises because dominant scattering typically occurs at small angles (roughly 50% in the forward direction between 0 and 2–6°) making it difficult to sense the weak scattering light, which is near the intense illuminating beam. Ideally, measurements should be done at several angles to better resolve the function. However, the backscatter signal, b_b, can be estimated with a few measurement angles provided the form of the volume scattering function is relatively well known. Recently developed volume scattering and backscatter instruments take advantage of this function. An important consideration is that backscattering is related to the size distribution, shapes, and composition of the particles sampled (e.g., coastal versus open ocean particles). Thus, this type of information can be obtained in principle. Radiative transfer models need both absorption and volume scattering function information to estimate the propagation of light. Also, an important remote sensing parameter, remote sensing reflectance (discussed below) is related to b_b and a. Key wavelengths are selected for the spectral measurements on the basis of the application and water types (e.g., coastal versus open ocean). Particle size distributions can also be measured using laser (Frauenhofer) diffraction instruments. These devices employ charged coupled device (CCD) array photodetectors (linear or circular ring geometries). Modified versions of some of these instruments can also measure particle settling velocities. Particles in the range of 5–500 μm can be measured with resolution dependent on the number of individual detector rings. These devices can also measure beam transmission by sensing the undeviated light.

Irradiance is the radiant flux per unit surface area (units of W m^{-2} or quanta (or photons) s^{-1} m^{-2} or mol quanta (or photons) s^{-1} m^{-2}. Note that 1 mol of photons is 6.02×10^{23} (Avogadro's number) and that one mole of photons is commonly called an einstein. It is convenient to define downwelling irradiance, E_d, as the irradiance of a downwelling light stream impinging on the top face of a horizontal surface (e.g., ideally flat light collector oriented perpendicular to the local gravity vector) and upwelling irradiance, E_u, as the irradiance of an upwelling light stream impinging on the bottom face of a horizontal surface. Irradiance reflectance, R, is E_u/E_d. Irradiance measurements are fundamentally important for quantifying the amount of light available for photosynthesis and for radiative transfer theory and computations. Another useful radiometric variable is radiance, $L = L(\theta,\Phi)$, which is defined as the radiant flux at a specified point in a given direction per unit solid angle per unit area perpendicular to the direction of light propagation (units of W (or quanta s^{-1}) m^{-2} sr^1). Zenith angle, θ, is the angle between a vertical line perpendicular to a flat plane and an incident light beam, and azimuthal angle, Φ, is the angle with respect to a reference line in the plane of the flat plate. By integrating $L(\theta,\Phi)\cos\theta$ over the solid angle ($d\omega = \sin\theta\ d\theta\ d\Phi$), of the upper hemisphere (say of a flat plate from $\theta = 0$ to $\pi/2$ and Φ from 0 to 2π), one obtains E_d. Similarly, upwelling irradiance, E_u, is calculated by integrating over the bottom hemisphere. Net downward irradiance is the difference $E_d - E_u$, or the integral of $L(\theta,\Phi)\cos\theta$ over the entire sphere (full solid angle 4π). Scalar irradiance, E_0, is defined as the integral of $L(\theta, \Phi)$ over the entire sphere. It should be noted that all definitions are for a specific wavelength of light. If one integrates scalar irradiance over the visible wavelengths (roughly 400–700 nm; note that the visible range is sometimes defined as 350–700 nm), then the biologically important quantity called photosynthetically available radiation (PAR) is obtained.

Apparent optical properties (AOPs) depend on both the IOPs and the angular distribution of solar radiation (i.e., the geometry of the subsurface ambient light field). To a reasonable approximation, the attenuation of spectral downwelling incident solar irradiance, $E_d(\lambda, z)$, can be described as an exponential function of depth:

$$E_d(\lambda, z) = E_d(\lambda, 0^-)\exp[-K_d(\lambda, z)z] \qquad [4]$$

where z is the vertical coordinate (positive downward), $E_d(\lambda, 0^-)$ is the value of E_d just below the air–sea interface, and $K_d(\lambda, z)$ is the spectral diffuse attenuation coefficient of downwelling irradiance. $K_d(\lambda)$ (here depth dependence notation is suppressed for convenience) is one of the important AOPs. The contributions of the various constituents (e.g., water, phytoplankton, detritus, and gelbstoff) to $K_d(\lambda)$ are often represented in analogy to the absorption coefficients given in eqn [1]. This leads to the term 'quasi-inherent' optical property as it is suggestive that inherent optical properties, i.e., like $a_t(\lambda)$, are closely related to $K_d(\lambda)$, which is often described as a quasi-inherent optical property. However, a key point is that $K_d(\lambda)$ is in fact dependent on the ambient light field. Analogous spectral

attenuation coefficients are defined for diffuse upwelling irradiance, downwelling radiance, and upwelling radiance, $K_L(\lambda)$. It should be noted that for periods of low sun angle and/or when highly reflective organisms or their products (e.g., coccolithophores and coccoliths) are present, then multiple scattering becomes increasingly more important and simple relations between IOPs and AOPs break down. It is important to mention that spectral radiometric measurements of AOPs have been far more commonly made than measurements of IOPs.

The relationships between IOPs and AOPs are central to developing quantitative models of spectral irradiance in the ocean. Radiative transfer theory is used to provide a mathematical formalism to link IOPs and the conditions of the water environment and light forcing to the AOPs of the water column. One motivation of this research is the desire to predict AOPs given environmental forcing conditions and estimates or actual measurements of IOPs. Another related, inverse goal is to be able to estimate or determine the vertical (and ideally horizontal) structure of IOPs and their temporal variability given normalized water-leaving radiance, $L_{wn}(\lambda)$, measured remotely from satellite or airplane color imagers. The extrapolation of subsurface values of $L(\lambda)$ to the surface has been the subject of considerable research, because a major requirement of ocean color remote sensing is to match *in situ* determinations of those from satellite- or plane-based spectral radiometers which necessarily must account for the effects of clouds and aerosols. As mentioned above, the important remote sensing parameter, spectral radiance reflectance, $L_u(\lambda)/E_d(\lambda)$, has been found to be proportional $b_b/(a + b_b)$ or b_b/a from Monte Carlo calculations for waters characterized by b/a values ranging from 1.0 to 5.0. The spectral radiance reflectance evaluated just above the ocean surface is defined as the remote sensing reflectance $R_{rs}(\lambda)$. It should also be noted that remote sensing estimates of pigment (typically chlorophyll *a* or chlorophyll *a* + phaeopigments) concentrations use empirical relations involving ratios such as $L_{wn}(443\,\text{nm})/L_{wn}(550\,\text{nm})$ or $R_{rs}(490\,\text{nm})/R_{rs}(555\,\text{nm})$ or these ratios with other wavelength combinations.

One of the most commonly used instruments for measuring AOPs is a broadband scalar irradiance E_0 or PAR sensor, because of the need for determining the availability of light for phytoplankton and its relative simplicity. A spherical light collector made of diffusing plastic receives the light from approximately 4π sr. The light is transmitted via a fiberoptic connector or quartz light conducting rod to a photodetector which records an output voltage. The instrument is calibrated with a standard lamp. Analogous sensors use flat plate cosine or hemispherical collectors. Spectroradiometers are irradiance or scalar irradiance meters which use a variable monochromator placed between a light collector and the photodetector. Light separation can be achieved using sets of interference filters (usually 10 nm in bandwidth) selected for particular purposes (e.g., absorption peaks and hinge points for pigments). Alternatively, higher spectral resolution (~ 3 nm from 400 to 800 nm) can be achieved using grating monochromators. Cosine (flat-plate), spherical, or hemispherical collectors are used for several different measurements or calculations of the AOPs described above (e.g., E_d, L_u, K_d, etc.). Irradiance cosine collectors are designed such that their responses to parallel radiant flux should be proportional to the angle between the normal to the collector surface and the direction of the radiant flux. This is necessary as the angle between the incoming radiant flux and the collector is variable, as is the area of the projection. To account for the differences in refractive indices of air and water, an immersion correction factor (typically 1.3–1.4) is applied. It should be noted that radiance sensors are designed to accept light in a small solid angle (typically a viewing angle of a few degrees). Irradiance and radiance instruments are calibrated using well-characterized, standard light sources. Because of the growing concern about UV radiation, a number of instruments are designed to measure into the UV portion of the electromagnetic spectrum as well.

A grand challenge of oceanography is to greatly increase the variety and quantity of ocean measurements. Optical and other ocean measurements are expensive. Thus, a major goal is to develop new sensors and systems, which can be efficiently deployed from a host of available ocean platforms including ships, moorings, drifters, floats, and autonomous underwater vehicles (AUVs). A further need is to telemeter the data in near real-time. Ship-based observations are useful for detailed profiling (high vertical resolution), but moorings are better suited for high temporal resolution, long-term measurements. Drifters, floats, and AUVs can provide horizontal coverage unattainable from the other *in situ* platforms. Ultimately, all of these platforms, along with satellite- and plane-based systems, are needed to fill in the time–space continuum. Several optical systems, which have been used for mooring-based time series studies, are illustrated in **Figure 1**. These collective instrument systems include most of the sensors described earlier. The

sampling for these instruments is typically done every few minutes (in some cases once per hour) for periods of several months. At this point in time, biofouling, rather than power or data storage, is the limiting factor. However, even this aspect is becoming less problematic with several new antibiofouling methods. In addition, more optical sensors are being deployed from other emerging platforms such as AUVs. The optimal utilization of optical data from the various platforms will require the use of advanced data merging methods and data assimilation models for predictions.

Optical Experiment Data Sets

Finally, a few examples of data, which have been collected with some of the optical instruments described above (**Figure 1**), are presented. An interdisciplinary experiment devoted to the understanding of relations between mixing processes and optical variability was conducted south of Cape Cod, Massachusetts on the continental shelf. Several spectral optical instruments collected IOP and AOP data sets using ship-based profiling and towed systems, moorings, and bottom tripods. The period of the experiment covered almost one year (July

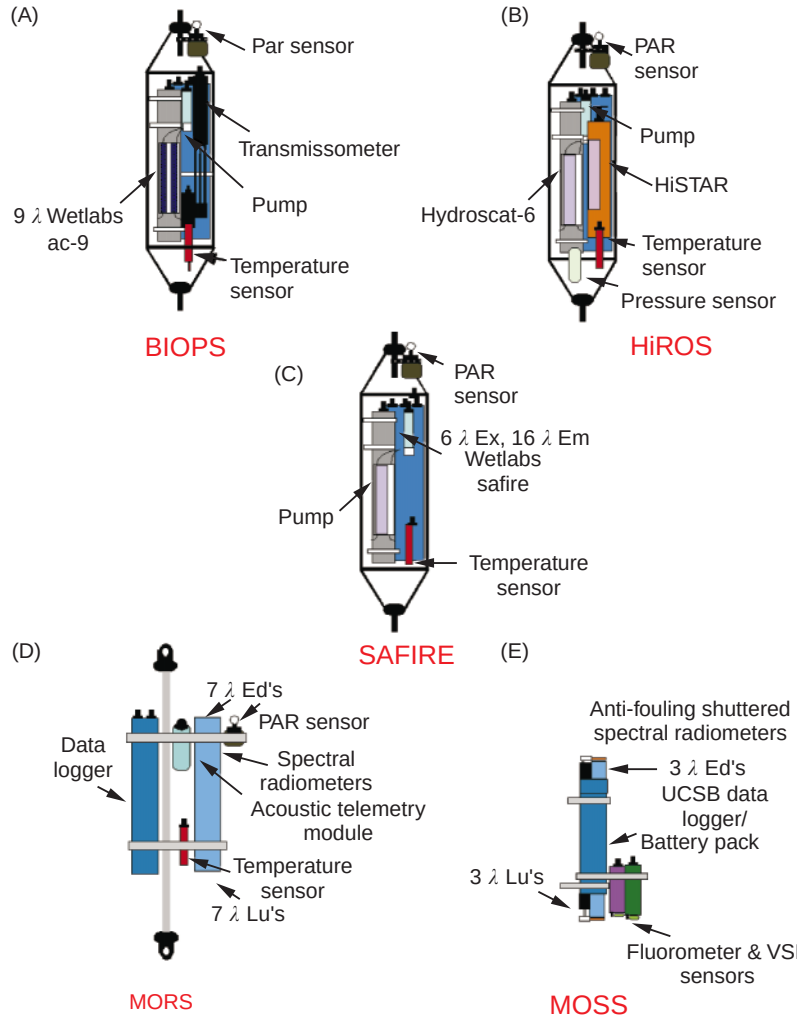

Figure 1 Schematic showing a variety of optical systems for mooring applications. (A) System used for measuring inherent optical properties (IOPs) including beam c (660 nm), spectral attenuation and absorption coefficients at nine wavelengths, along with PAR and temperature. (B) System used for measuring inherent optical properties including spectral attenuation and absorption coefficients at 100 wavelengths, spectral backscatter at six wavelengths, along with PAR, temperature, and pressure. (C) System measuring spectral fluorescence with 6 excitation wavelengths and 16 emission wavelengths; also PAR and temperature sensors are included. (D) System for measuring apparent optical properties (AOPs) including spectral downwelling irradiance and upwelling radiance at seven wavelengths and PAR along with temperature. A telemetry module is also included. (E) System for measuring apparent optical properties (AOPs) including spectral downwelling irradiance and upwelling radiance at three wavelengths along with instruments for measuring chlorophyll fluorescence, volume scattering function. An antifouling shutter system is also utilized.

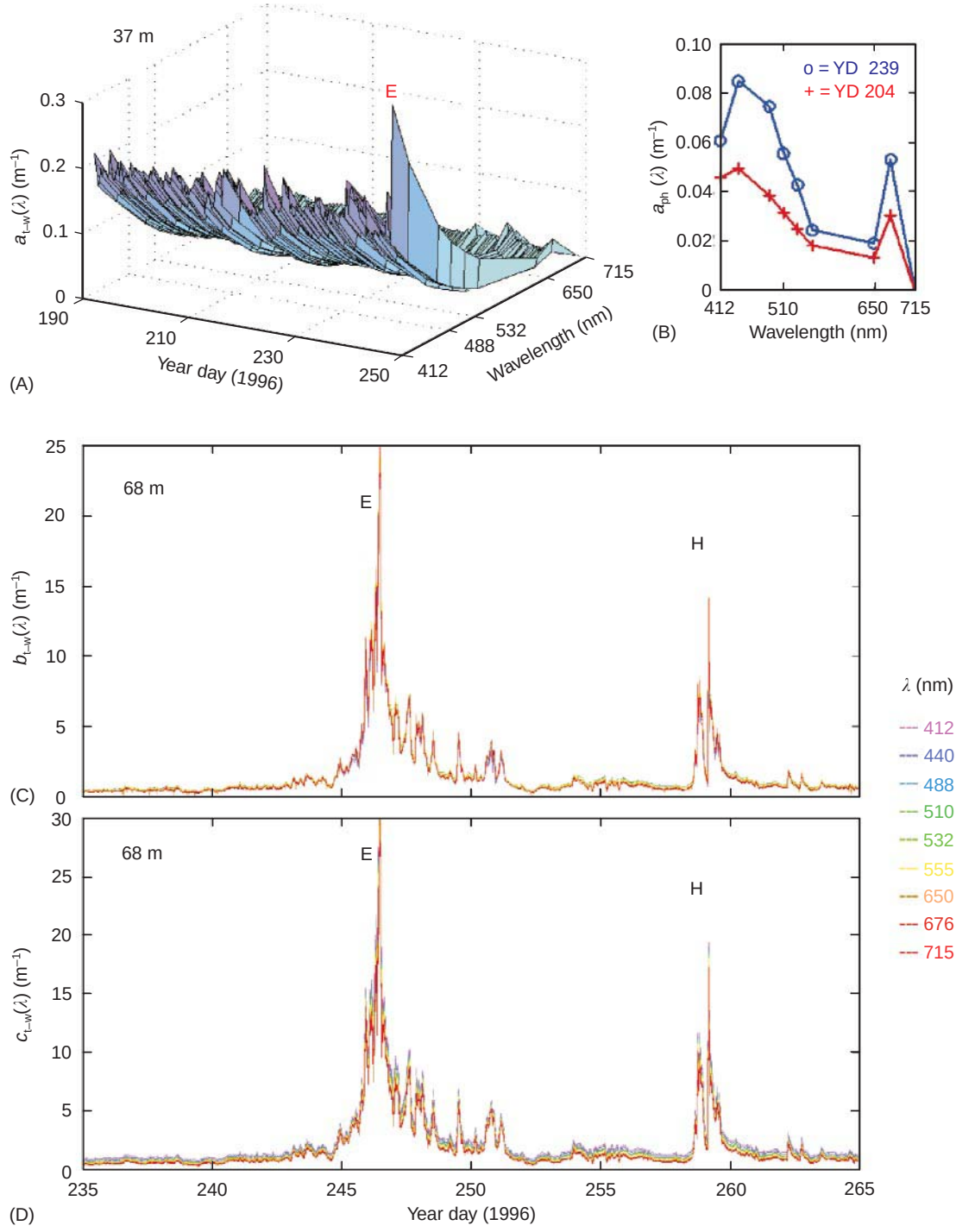

Figure 2 Illustrations showing data collected from the BIOPS system shown in **Figure 1**(**A**) on the continental shelf south of Cape Cod Massachusetts in the summer and fall of 1996. (A) A time series of the total spectral absorption coefficient of light (after subtracting the clear water component) at a depth of 37 m (total water depth is 70 m). (B) The spectral absorption on YD 204 and 239. (C) Time series of spectral scattering coefficient computed by differencing the total spectral attenuation and absorption coefficients (again, the clear water coefficient has been subtracted) at 68 m. The large peaks are attributed to passages of hurricanes Edouard (E) and Hortense (H). (D) as for (C) except for spectral beam attenuation coefficients. (Figures based on Chang and Dickey, 1999.)

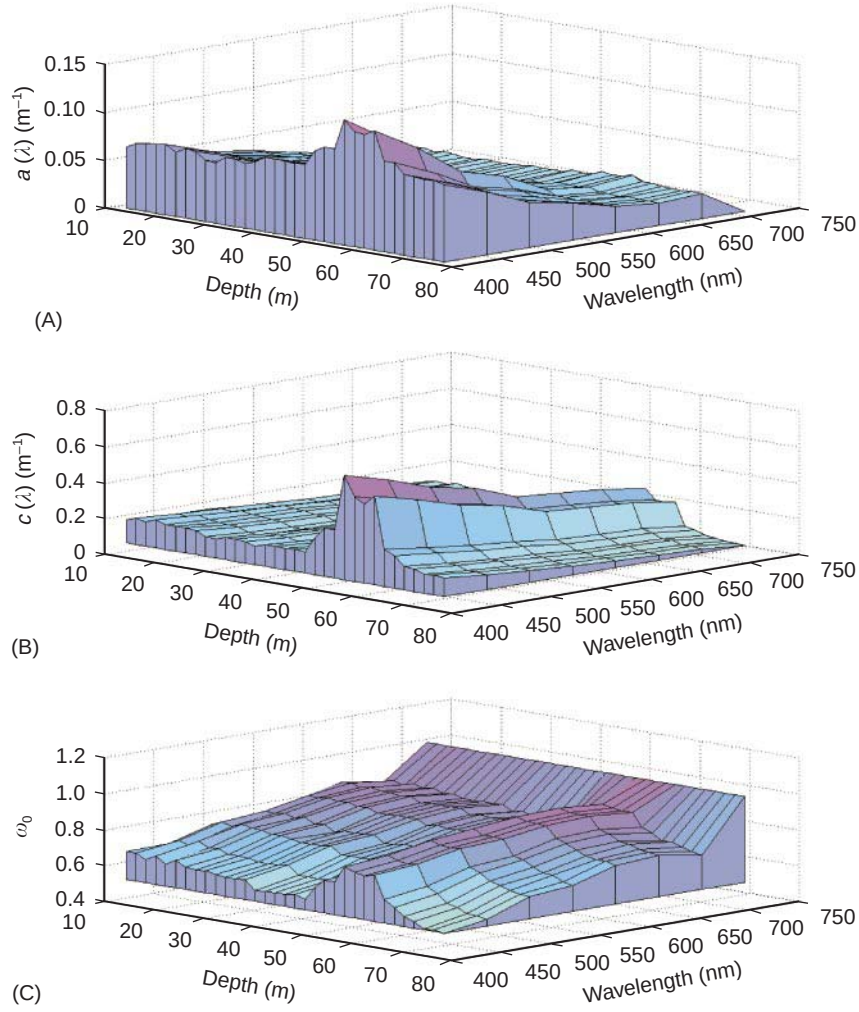

Figure 3 Data collected near an ocean sewage outfall in Mamala Bay off Honolulu, Hawaii in the fall of 1994. Vertical profiles of (A) spectral absorption coefficient, (B) spectral attenuation coefficient, and (C) single scattering albedo. Data were obtained from an ac-meter system similar to the one shown in **Figure 1**(**A**). Eight wavelengths are displayed and the major peak near 60 m is caused by sewage plume waters with high scattering and absorption coefficents. (Figures based on Petrenko *et al.*, 1997.)

1996–June 1997). Some instruments sampled at several minute to hourly intervals whereas others sampled with vertical resolution on the scale of centimeters for a few weeks during two intensive field campaigns. Several interesting observations were enabled. These included: sediment resuspension forced by two passing hurricanes (hurricane Edouard and hurricane Hortense), spring and fall phytoplankton blooms, water mass intrusions, and internal solitary waves. Time series data collected using the BIOP system (e.g., BIOPS and MORS in **Figure 1**) which was deployed from a mooring and a bottom tripod located near each other in 70 m waters, are shown in **Figure 2**. **Figure 2**(**A**) shows the 37-m time series of total spectral absorption (water absorption has been subtracted) using a nine-wavelength ac-meter. The major feature is related to hurricane Edouard. The spectral absorption contributions due to phytoplankton are shown for two days in the summer in **Figure 2**(**B**); the peaks at 440 and 683 nm are caused by phytoplankton. **Figure 2**(**C, D**) shows ac-meter time series of spectral (nine wavelengths) scattering and attenuation coefficients. The record is dominated by sediment resuspension caused by mixing and waves created by hurricane Edouard and the more distant hurricane Hortense. The complete mooring data set showed that sediments were lifted more than 30 m above the ocean floor.

The second example highlights optical data collected from a ship-based profiling system (similar to the system shown in **Figure 1A**). The purpose of the

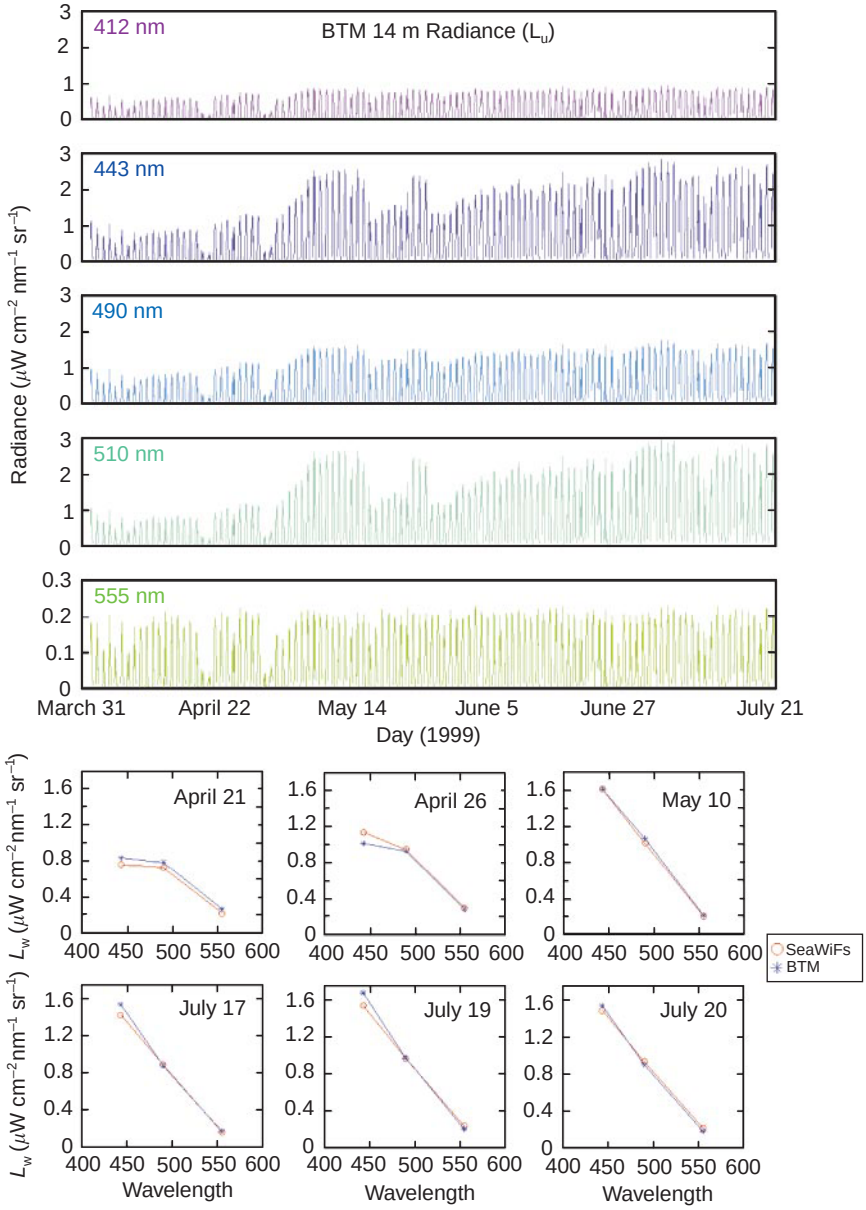

Figure 4 BTM radiometer data collected with the system shown in **Figure 1**(**D**). The top set of panels shows a time series of spectral upwelling radiance (five wavelengths) from the 14-m spectral radiometer system (April–July, 1999). The bottom set of panels shows spectral water-leaving radiance derived from the BTM radiometers and from the SeaWiFS ocean color satellite for six days of the sampling period.

measurements was to study the dispersion of contaminants (treated wastewaters) discharged about 4 km offshore (70 m water depth) into Mamala Bay, off the coast of Honolulu, Hawaii in the fall of 1994. Optical and physical measurements were made from shipboard using both profile and towing modes in the vicinity of the outfall plume. Optical instrumentation included a beam transmissometer (660 nm), spectral ac-meters (nine wavelengths for *a* and *c*), PAR sensor, chlorophyll fluorometer, a particle size analyzer (laser diffraction method), and a spectral absorption and fluorescence instrument. Physical measurements of temperature, salinity and pressure were also done. Sampling was designed to track both the horizontal and vertical structure of effluent as manifest in the optical signals. The water contributions to *a*, *b*, and *c* were removed for the analyses. The collective optical and physical measurements enabled the partitioning of particle types into categories: particulate versus

dissolved components, phytoplankton opposed to detrital components, shallow layer versus deep layer phytoplankton, and old versus newly discharged sewage plume waters. Briefly, a profile (see **Figure 3**) taken near the end of the outfall diffuser (water depth $\sim$ 80 m) displayed the following features: (1) sewage plume waters centered near 60 m as characterized by low salinity and very high values of spectral attenuation and absorption (greater in the shorter wavelengths), and (2) a shallow phytoplankton layer near 20 m with modest relative maxima in chlorophyll fluorescence and spectral absorption and attenuation coefficients in the blue. The profile of spectral single-scattering albedo, $\omega_0(\lambda) = b(\lambda)/c(\lambda)$, shows a general trend of increased importance of scattering for greater wavelengths with the most pronounced effect for the sewage plume waters centered at 60 m (**Figure 3C**).

The final example describes an important linkage between *in situ* and remote sensing observations of ocean color. The Bermuda Testbed Mooring (BTM) is used to test new oceanographic instrumentation (including systems shown in **Figure 1**), for scientific studies devoted to biogeochemical cycling and climate change, and for groundtruthing (verification using *in situ* data) and algorithm development for ocean color satellites such as SeaWiFS. The latter aspect is the focus here. Two BTM optical systems utilizing radiometers for measurements of spectral downwelling irradiance and spectral upwelling radiance are illustrated in **Figure 1**(**D**) and (**E**). These systems measure at wavelengths, which are coincident with those of the SeaWiFS ocean color satellite, and sample at hourly intervals. Two or more systems are deployed at different depths and another radiometer system is deployed from the surface buoy to collect incident spectral downwelling irradiance. Derived quantities include time series of several of the AOP quantities introduced earlier (e.g., spectral diffuse attenuation coefficients, spectral reflectances including remote sensing reflectance, and water-leaving radiance). Time series of spectral upwelled radiance from the BTM radiometer system (**Figure 1D**) located at 14 m are shown for the period April through July, 1999 in the top set of panels of **Figure 4**. The variability is primarily caused by the daily cycle of solar insolation, cloud cover, and optical properties associated with phytoplankton and their products. The bottom panels of **Figure 4** show a subset of the water-leaving radiance data as determined from the BTM radiometers (extrapolation to surface) and SeaWiFS satellite sensors for six days during the particular sampling period. These two types of data are critical for quantifying both the temporal and horizontal spatial variability of water clarity, PAR, phytoplankton biomass, and primary productivity.

Toward the Future

The last two decades have been marked by the emergence of a host of new optical instruments and systems; their applications are growing at a rapid rate. Looking toward the future, it is anticipated that optical instrumentation will be (1) more capable in spectral resolution, (2) smaller and require less power, (3) suitable for deployment from a variety of autonomous platforms, (4) designed for ease in telemetering of data for real-time applications, and (5) less costly as demand increases enabling higher volumes of data collection.

See also

Absorbance Spectroscopy for Chemical Sensors. Autonomous Underwater Vehicles (AUVs). Bioluminescence. Drifters and Floats. IR Radiometers. Ocean Color from Satellites. Optical Particle Characterization. Penetrating Shortwave Radiation. Satellite Remote Sensing Microwave Scatterometers.

Further Reading

Agrawal YC and Pottsmith HC (1994) Laser diffraction particle sizing in STRESS. *Continental Shelf Research* 14: 1101–1121.

Bartz R, Zaneveld JRV and Pak H (1978) A transmissometer for profiling and moored observations in water. *Ocean Optics V*, *SPIE* 160: 102–108.

Booth CR (1976) The design and evaluation of a measurement system for photsynthetically active quantum scalar irradiance. *Limnology and Oceanography* 19: 326–335.

Chang GC and Dickey TD (1999) Partitioning *in situ* total spectral absorption by use of moored spectral absorption and attenuation meters. *Applied Optics* 38: 3876–3887.

Chang GC and Dickey TD (2001) Optical and physical variability on time-scales from minutes to the seasonal cycle on the New England continental shelf: July 1996–June 1997. *Journal of Geophysical Research* 106: 9435–9453.

Chang GC, Dickey TD and Williams AJ 3rd (2001) Sediment resuspension over a continental shelf during Hurricanes Edouard and Hortense. *Journal of Geophysical Research* 106: 9517–9531.

Dana DR, Maffione RA and Coenen PE (1998) A new *in situ* instrument for measuring the backward scattering and absorption coefficients simultaneously. *Ocean Optics XIV* 1: 1–8.

Dickey T (1991) Concurrent high resolution physical and bio-optical measurements in the upper ocean and their applications. *Reviews in Geophysics* 29: 383–413.

Dickey T, Granata T, Marra J *et al.* (1993) Seasonal variability of bio-optical and physical properties in the Sargasso Sea. *Journal of Geophysical Research* 98: 865–898.

Dickey T, Marra J, Stramska M *et al.* (1994) Bio-optical and physical variability in the sub-arctic North Atlantic Ocean during the spring of 1989. *Journal of Geophysical Research* 99: 22541–22556.

Dickey T, Frye D, Jannasch H *et al.* (1998) Initial results from the Bermuda Testbed Mooring Program. *Deep-Sea Research I* 45: 771–794.

Dickey T, Marra J, Weller R *et al.* (1998) Time-series of bio-optical and physical properties in the Arabian Sea: October 1994–October 1995. *Deep-Sea Research II* 45: 2001–2025.

Dickey TD, Chang GC, Agrawal YC, Williams AJ 3rd and Hill PS (1998) Sediment resuspension in the wakes of Hurricanes Edouard and Hortense. *Geophysical Research Letters* 25: 3533–3536.

Dickey T, Zedler S, Frye D *et al.* (2001) Physical and biogeochemical variability from hours to years at the Bermuda Testbed Mooring site: June 1994–March 1998. *Deep-Sea Research*.

Foley D, Dickey T, McPhaden M *et al.* (1998) Longwaves and primary productivity variations in the equatorial Pacific at 0°, 140°W February 1992–March 1993. *Deep-Sea Research II* 44: 1801–1826.

Gentien P, Lunven M, Lehaitre M and Duvent JL (1995) *In situ* depth profiling of particle sizes. *Deep-Sea Research* 42: 1297–1312.

Griffiths G, Knap A and Dickey T (1999) Autosub experiment near Bermuda. *Sea Technology*, December.

Jerlov NG (1976) *Marine Optics*. Amsterdam: Elsevier.

Kirk JTO (1994) *Light and Photosynthesis in Aquatic Ecosystems*, 2nd edn. Cambridge: Cambridge University Press.

Mobley CD (1994) *Light and Water: Radiative Transfer in Natural Waters*. San Diego: Academic Press.

Moore CC, Zaneveld JRV and Kitchen JC (1992) Preliminary results from *in situ* spectral absorption meter data. *Ocean Optics XI, SPIE* 1750: 330–337.

O'Reilly JE, Maritorena S, Mitchell BG *et al.* (1998) Ocean color chlorophyll algorithms for SeaWiFS. *Journal of Geophysical Research* 103: 24937–24953.

Petrenko AA, Jones BH, Dickey TD, Le Haitre M and Moore C (1997) Effects of a sewage plume on the biology, optical characteristic and particle size distributions of coastal waters. *Journal of Geophysical Research* 102: 25 061–25 071.

Petrenko AA, Jones BH and Dickey TD (1998) Shape and near-field dilution of the Sand Island sewage plume: observations compared to model results. *Journal of Hydraulic Engineering* 124: 565–571.

Petzold, TJ (1972) Volume scattering functions for selected waters, Scripps Institution of Oceanography Reference 72–78. La Jolla, California: Scripps Institution of Oceanography.

Smith RC, Booth CR and Star JL (1984) Oceanographic bio-optical profiling system. *Applied Optics* 23: 2791–2797.

Spinrad RW, Carder KL and Perry MJ (1994) *Ocean Optics*. Oxford: Oxford University Press.

INTERNAL TIDAL MIXING

W. Munk, University of California San Diego, La Jolla, CA, USA

doi:10.1006/rwos.2001.0139

Introduction

Any meaningful attempt towards understanding how the ocean works has to include an allowance for mixing processes. A great deal is known about the transport of heat and solutes by molecular processes in laboratory-scale experiments. Quite naturally, at the dawn of ocean science, these concepts were borrowed to speculate about the oceans. On that basis it was suggested by Zoeppritz that the temperature structure T(z) at 1000 m depth could be interpreted in terms of the time history T(t) at the surface some 10 million years earlier. It would indeed be nice if past climate could be inferred in this simple manner.

Once it was realized that molecular diffusion failed miserably to account for the transports of heat and salt, generations of oceanographers attempted to patch up the situation by replacing the molecular coefficients of conductivity and diffusivity by enormously larger eddy coefficients, but leaving the governing laws (equations) unchanged. By an arbitrary choice of the magnitude of the coefficients it was generally possible to achieve a satisfactory (to the author) agreement between theory and observation, a result aided by the uncertainty of the measurements. But the clear danger signal was there; each experiment, each process required a different set of values.

The present generation of oceanographers has come to terms with the need for understanding the mixing processes, just as they had come to terms